

Nomograms for Rapid Evaluation of Magnetic Anomalies Over Long Tabular Bodies

By D. ATCHUTA RAO and H. V. RAM BABU¹

Abstract – The magnetic anomaly due to a long tabular body usually consists of a maximum and a minimum. The distances and the amplitudes of the maximum and the minimum, when defined in dimensionless quantities, may be used as characteristics of the source. In this paper, a method based on the positions of the maximum and the minimum on the magnetic anomaly due to a long tabular body has been presented. Characteristic ratios, D and A involving the distances and amplitudes of the maximum and the minimum points on the anomaly curve are defined. Nomograms showing the variations of D and A with the parameters of (1) the dike and (2) the vertical fault models are presented. The parameters of the causative source are evaluated from the two ratios D and A and the nomograms, using some simple analytical relations presented here. From the nomograms, it is observed that (a) for a thick dike, A is always greater than D , (b) $A = D$ for a thin sheet and (c) for a vertical fault, A is always less than D . Thus from the characteristic ratios D and A it is possible to evaluate the source parameters and also to distinguish whether the source is a dike, sheet or a vertical fault. The method is fast and is applicable for the magnetic anomalies either in total, vertical or horizontal component. The method has been applied on two field examples and the results are found to be in close agreement with those obtained by using other methods. A simple method of locating the origin on the anomaly curve is included. The limitations of the method are also discussed.

Key words: Magnetic interpretation; Nomograms; Dike; Fault; Characteristic curves.

1. Introduction

Analysis of magnetic anomalies by the use of characteristic curves is one of the classical methods of interpretation. AM (1972) in a critical review of the existing methods of analysis using characteristic curves (BRUCKSHAW and KUNARATNAM, 1963; MOO, 1965; BEAN, 1966; GRANT and MARTIN, 1966 etc.) mentioned that the characteristic points chosen should be:

- (1) based on lengths which can be readily identified,
- (2) extending not too far out on the sides of anomaly and
- (3) obtained rapidly not involving too much calculation.

The above three conditions are satisfied by the maximum and the minimum points on the magnetic anomaly curve due to a long tabular body, in intermediate latitudes. In this

¹ National Geophysical Research Institute, Hyderabad – 500 007, India.

paper, two ratios D and A are defined and used as characteristics of the source parameters. Variation of D with A for different combinations of body parameters are presented in the form of nomograms for dike and vertical fault models.

2. Theory

In formulating the magnetic anomalies due to (1) dike and (2) vertical fault models, the following notation has been used. In an XOY cartesian co-ordinate system (Fig. 1a) the Y -axis is chosen along the strike of the body. The magnetic profile is along the X -axis, making an angle α with the magnetic north. I_0 is the inclination of the earth's magnetic field of intensity T . J_0 and a are the inclination and declination of the resultant magnetization J (in case when the body is permanently magnetized). K is the susceptibility contrast of the body to its surroundings. I'_0 and J'_0 are the effective inclination of the induced and the resultant field respectively and are given by (after HOOD, 1964)

$$\tan I'_0 = \frac{\tan I_0}{\cos \alpha} \quad \text{and} \quad \tan J'_0 = \frac{\tan J_0}{\cos \alpha}$$

(a) The dike model

The general expression for the magnetic anomaly $[\Delta F]$ at any point $M(x)$ along a traverse perpendicular to the strike of a two-dimensional dipping dike (Fig. 1b) of infinite depth extent [following equation (22) of GAY (1963)] is

$$\Delta F = C \left[\sin \theta \cdot \log_e \left\{ \frac{(x+b)^2 + h^2}{(x-b)^2 + h^2} \right\}^{1/2} + \cos \theta \left\{ \tan^{-1} \frac{x+b}{h} - \tan^{-1} \frac{x-b}{h} \right\} \right] \quad (1)$$

Where, x is the distance of the point of observation from the origin, h is the depth to the top of the dike, C and θ are the amplitude coefficient and the index parameter whose equivalents are given in Table 1 for the three cases of ΔF .

Expressing x and b in depth units, equation (1) may be rewritten as

$$\Delta F = C \left[\sin \theta \cdot \log_e \left\{ \frac{(X+R/2)^2 + 1}{(X-R/2)^2 + 1} \right\}^{1/2} + \cos \theta \left\{ \tan^{-1}(X+R/2) - \tan^{-1}(X-R/2) \right\} \right] \quad (2)$$

where, $X = x/h$ and $R = 2b/h$.

From equation (2) the condition for maxima/minima on ΔF is

$$X^2 + 2X \cot \theta - (1 + R^2/4) = 0 \quad (3)$$

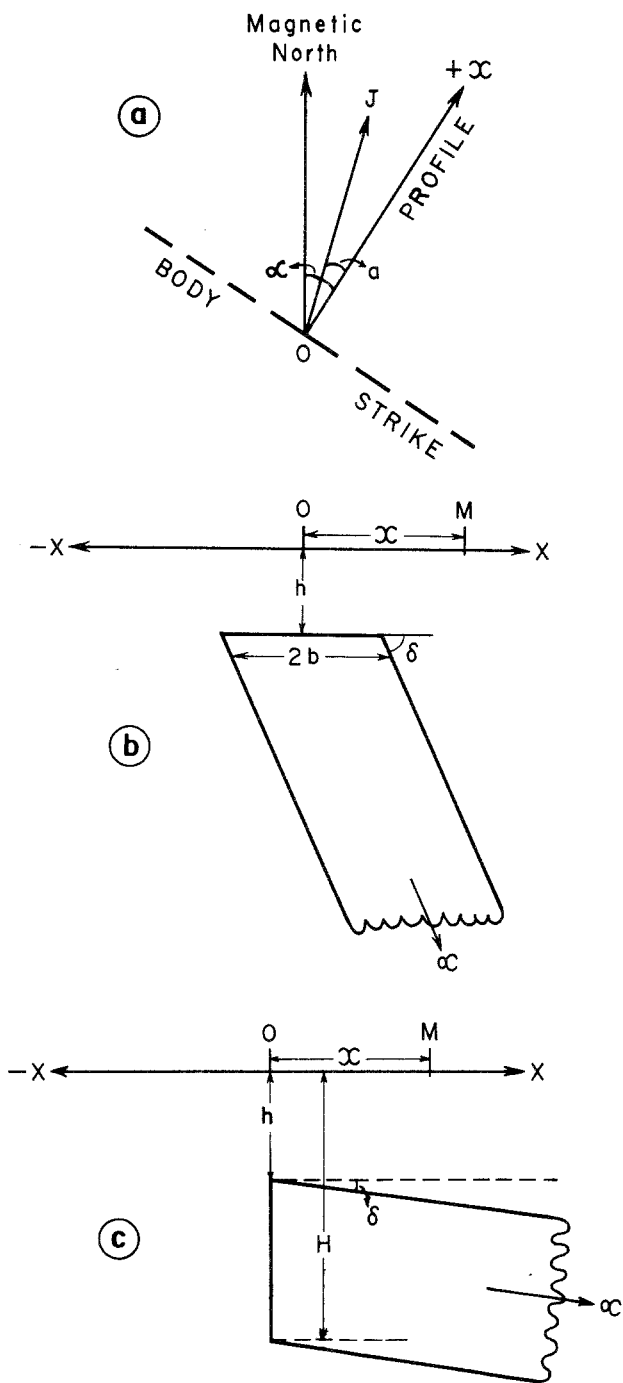


Figure 1

(a) Notations used in the derivation of anomalies, (b) cross-sectional view of a dike and (c) cross-sectional view of a vertical fault.

Table 1

Equivalents of the amplitude coefficient, C and the index parameter, θ for a dike/vertical fault magnetized due to induction or remanence. $B = \sin \delta$ for dike and $B = \cos \delta$ for vertical fault. For induced magnetization, $J_0 = I_0$; $a = \alpha$; $J'_0 = I'_0$ and $P = KT$

Anomaly in	Amplitude coefficient C	Index parameter θ
Total field	$2PB(1 - \cos^2 I_0 \sin^2 \alpha)^{1/2} \cdot (1 - \cos^2 J_0 \sin^2 a)^{1/2}$	$I_0 + J'_0 - \delta - 90^\circ$
Vertical field	$2PB(1 - \cos^2 J_0 \sin^2 a)^{1/2}$	$J'_0 - \delta$
Horizontal field	$2PB \sin \alpha (1 - \cos^2 J_0 \sin^2 a)^{1/2}$	$J'_0 - \delta - 90^\circ$

The two roots of equation (3) correspond to the maximum (X_M) and the minimum (X_m) points on ΔF and are given by

$$X_M = -\cot \theta + \sqrt{\operatorname{cosec}^2 \theta + R^2/4} \tag{4}$$

and

$$X_m = -\cot \theta - \sqrt{\operatorname{cosec}^2 \theta + R^2/4} \tag{5}$$

Let

$$\left| \frac{X_M + X_m}{X_M - X_m} \right| = D \tag{6}$$

then we have from equations (4) and (5)

$$D = \left| \frac{2 \cos \theta}{\sqrt{4 + R^2 \sin^2 \theta}} \right| \tag{7}$$

It is evident from equation (7) that the ratio D depends on R and θ only.

Let us define another ratio A such that

$$A = \left| \frac{F_M + F_m}{F_M - F_m} \right| \tag{8}$$

where

$$F_M = C \left[\sin \theta \cdot \log_e \left\{ \frac{(X_M + R/2)^2 + 1}{(X_M - R/2)^2 + 1} \right\}^{1/2} + \cos \theta \{ \tan^{-1}(X_M + R/2) - \tan^{-1}(X_M - R/2) \} \right] \tag{9}$$

and

$$F_m = C \left[\sin \theta \cdot \log_e \left\{ \frac{(X_m + R/2)^2 + 1}{(X_m - R/2)^2 + 1} \right\}^{1/2} + \cos \theta \{ \tan^{-1}(X_m + R/2) - \tan^{-1}(X_m - R/2) \} \right] \tag{10}$$

in which X_M and X_m are defined by equations (4) and (5). Substituting equations (9) and (10) in equation (8) and simplifying, we get

$$A = a_1/a_2 \tag{11}$$

where

$$a_1 = 2 \cos \theta \cdot \tan^{-1}(R/2) \tag{12}$$

and

$$a_2 = 0.5 \sin \theta \cdot \log_e \frac{2 + R^2 \sin^2 \theta + R \sin \theta (4 + R^2 \sin^2 \theta)^{1/2}}{2 + R^2 \sin \theta - R \sin \theta (4 + R^2 \sin^2 \theta)^{1/2}} + \cos \theta \cdot \tan^{-1} \left[\frac{2R \cos \theta \cdot (4 + R^2 \sin^2 \theta)^{1/2}}{4 + R^2(\sin^2 \theta - \cos^2 \theta)} \right] \tag{13}$$

It may be seen from equation (11) that the ratio A depends on R and θ of the dike. Thus both the ratios A and D depend on R and θ only and may be used as characteristics of the dike. In a plot of D versus A for various combinations of R and θ , a pair of D and A values correspond to a single set of R and θ . We adopt this principle in the construction of nomograms presented in Fig. 2.

Limits for D and A: From equation (7) we have that $D = 1$ when $\theta = 0^\circ$ and $D = 0$ when $\theta = 90^\circ$. Thus the limits for D are

$$0 \leq D \leq 1$$

Similarly, the limits for A are

$$0 \leq A \leq 1$$

Preparation of nomograms: Nomograms showing the variation of A with D for different values of R and θ are presented in Fig. 2. These curves are prepared for $R = 0, 1, 2, 3, 4, 5, 6, 8, 10, 15$ and 20 . The index parameter, θ is varied between 0° and 90° only because the ΔF curves outside this range are all mirror images of those in this range (0° to 90°). When $R = 0$ (i.e., thin dike case), it is easy to prove that $D = A$ for any value of θ . Hence the plot of D versus A for $R = 0$ is a straight line whose slope is unity (see $R = 0$ curve in Fig. 2).

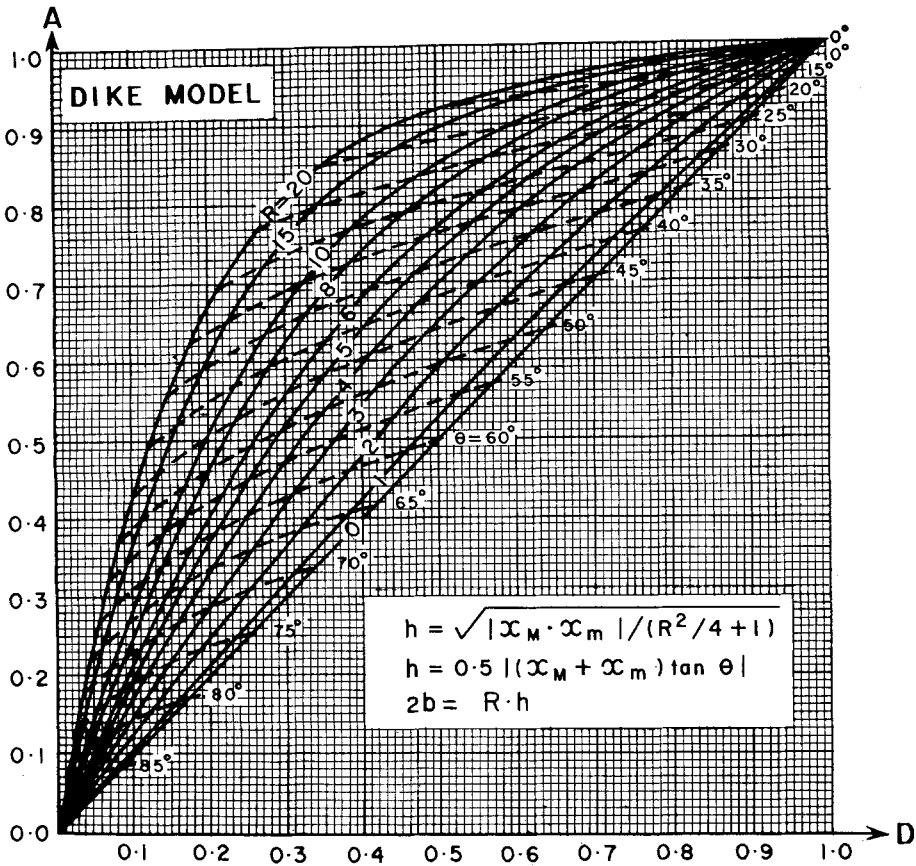


Figure 2

Nomograms for the dike model showing the relation between the characteristic ratios D and A for different values of R and θ .

(b) *The vertical fault model*

Similar to the dike anomaly, the magnetic anomalies in the three components along a traverse perpendicular to the strike of a vertical fault (Fig. 1c) belong to a single family and may be represented by the general expression

$$\Delta F = C \left[\cos \theta \cdot \log_e \left(\frac{x^2 + H^2}{x^2 + h^2} \right)^{1/2} + \sin \theta \cdot \left(\tan^{-1} \frac{x}{h} - \tan^{-1} \frac{x}{H} \right) \right] \quad (14)$$

where, h and H are the depths to the top and bottom edges of the fault. The equivalents of C and θ are given in Table 1 for the three cases of ΔF .

Using the same definitions of D and A as given in equations (6) and (8) we have for the vertical fault

$$D = \left| \frac{(R + 2) \cos \theta}{\sqrt{(R + 2)^2 \cos^2 \theta + 4(R + 1) \sin \theta}} \right| \quad (15)$$

and

$$A = b_1/(b_2 + b_3) \quad (16)$$

where

$$b_1 = \cos \theta \cdot \log_e (R + 1) \quad (17)$$

$$b_2 = 0.5 \cos \theta \cdot \log_e \frac{b_{21} + b_{22}}{b_{21} - b_{22}} \quad (18)$$

$$b_{21} = 2(R + 1)^2 + 0.5(R^2 + 2R + 2) \{(R + 2)^2 \cot^2 \theta + 2(R + 1)\}, \quad (18a)$$

$$b_{22} = 0.5 \cot \theta \cdot R(R + 2)^2 \{(R + 2)^2 \cot^2 \theta + 4(R + 1)\}^{1/2} \quad (18b)$$

and

$$b_3 = \sin \theta \cdot \tan^{-1} \left[\frac{2R \{(R + 2)^2 \cot^2 \theta + 4(R + 1)\}^{1/2}}{(R + 2)^2 \cot^2 \theta + 4(R + 1) - R^2} \right] \quad (19)$$

It is evident from equations (15) and (16) that the two ratios D and A depend on R and θ only and may be used as characteristics of the fault.

It is easy to show that the same limits obtained for D and A for the dike model are also valid for the vertical fault.

Variation of A with D for different combinations of R and θ is presented in the form of nomograms in Fig. 3. These nomograms are prepared for the following values of R and θ . R is given the values 0, 1, 2, 3, 4, 5, 6, 8, 10, 15 and 20. The angle θ is varied in the range 0° to 90° only because the ΔF curves outside this range are all mirror images of those in this range. The nomogram for $R = 0$ (Fig. 3) belongs to the thin sheet case.

(c) Comparison of nomograms for dike and vertical fault models

The following qualitative comparison between the nomograms for dike and vertical fault models may be made from Figs. 2 and 3. (i) The nomograms for the dike model, when $R > 0$, are characterized by the ratios A and D in which A is always greater than D . The nomogram $R = 0$ in which $A = D$ is indicative of a thin sheet. (ii) The nomograms for the fault model, when $R > 0$ are characterized by the ratios A and D in which A is always less than D . Thus the ratios A and D may be used to distinguish whether the causative source is a dike, sheet or a vertical fault.

3. Interpretational procedure

(a) Magnetic parameters

First, the magnetic inclination (I_0) and the base level of the total field (T) in the area of survey are noted. The azimuth (α) of the profile is measured in the clockwise

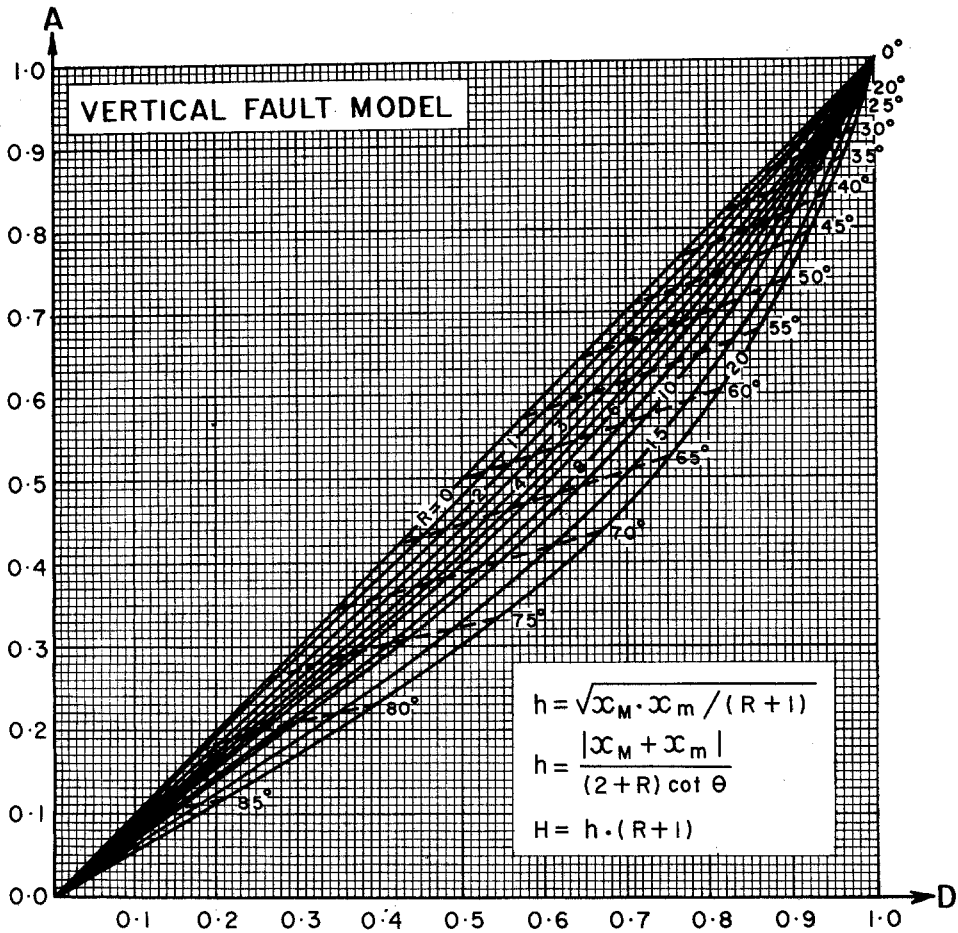


Figure 3

Nomograms for the vertical fault model showing the relation between the characteristic ratios D and A for different values of R and θ .

direction from magnetic north. The effective inclination (I'_0) may be calculated using the relation $I'_0 = \arctan(\tan I_0 / \cos \alpha)$.

(b) Location of the origin and the zero line

For a field curve, both the origin and the zero line are unknown. They may be determined using POWELL's (1967) method, Lamontagne's (KOULOMZINE *et al.*, 1970) method or the method presented below.

Let there be two points P and Q at distances x_1 and x'_1 on ΔF curve (Fig. 4) such that

$$\Delta F(x_1) = \Delta F(x'_1) = F_M - \delta F = F_1$$

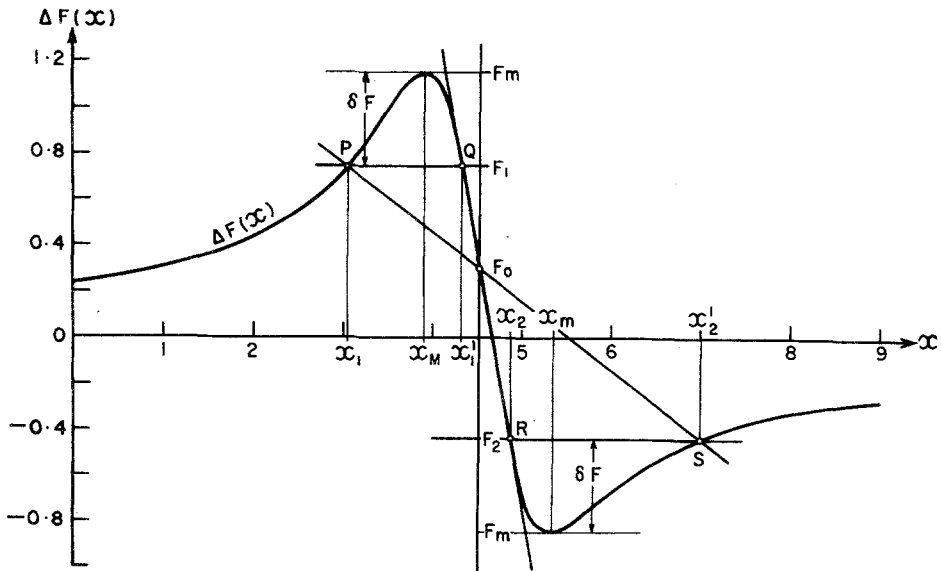


Figure 4

Anomaly curve $[\Delta F(x)]$ showing the characteristic amplitudes and distances (in arbitrary units) used in the analysis. The points P, Q, R and S are used to locate the origin. The origin will be directly below the intersection point of the lines PS and QR .

and two other points R and S at distances x_2 and x'_2 such that

$$\Delta F(x_2) = \Delta F(x'_2) = F_m + \delta F = F_2$$

where $\delta F = (F_M - F_m)/N$, in which N is a number greater than unity. Now the co-ordinates of these points in the $x, \Delta F$ co-ordinate system are $P(x_1, F_1), Q(x'_1, F_1), R(x_2, F_2)$ and $S(x'_2, F_2)$. The equation for the straight line PS formed by joining the points P and S may be written as

$$\frac{x - x_1}{x'_2 - x_1} = \frac{\Delta F - F_1}{F_2 - F_1} \tag{20}$$

Similarly, the equation for the straight line QR formed by joining the points Q and R is

$$\frac{x - x'_1}{x_2 - x'_1} = \frac{\Delta F - F_1}{F_2 - F_1} \tag{21}$$

Eliminating ΔF in equations (20) and (21) we get the abscissa of the point at which the lines PS and QR intersect as

$$x = \frac{x_1 x_2 - x'_1 x'_2}{x_1 - x'_1 + x_2 - x'_2} \tag{22}$$

POWELL (1967, Fig. 2) has shown that $x_1 x_2 = x'_1 x'_2$ for both dike and vertical fault

models. Hence equation (22) reduces to $x = 0$, which indicates that the lines PS and QR intersect directly over $x = 0$, the origin.

After locating the origin, the zero line is determined using the well-known relation

$$F_M + F_m = F_0 \quad (23)$$

where F_0 is the amplitude of ΔF over the origin.

(c) *Determination of A and D*

The ratios A and D are found using the relations given in equations (6) and (8).

(d) *Identification of the causative source*

It may be inferred from the characteristic ratios A and D that the given ΔF curve belongs to the dike family if $A > D$, fault family if $A < D$ or thin sheet family if $A = D$.

(e) *Estimation of body parameters*

The characteristic ratios A and D are entered in to the nomograms for the dike model (Fig. 2) if $A \geq D$ or fault model (Fig. 3) if $A \leq D$ and the corresponding values of R and θ are noted. Using these values of R and θ the source parameters are determined using the analytical relations given below.

(i) *Dike model:* The depth (h) to the top may be found from either of the following two relations derived from equations (4) and (5).

$$h = 0.5 |(x_M + x_m) \cdot \tan \theta| \quad (24)$$

or

$$h = \sqrt{\left| \frac{x_M \cdot x_m}{(1 + R^2/4)} \right|} \quad (25)$$

The width ($2b$) of the dike is evaluated using the relation

$$2b = R \cdot h \quad (26)$$

Since, using Fig. 2 one obtains the θ value in the range 0° to 90° only, the actual value of θ may be found using the following criteria:

Major positive anomaly towards positive x -axis

$$\theta = \theta_N \quad \text{or} \quad \theta_N - 360^\circ;$$

Major positive anomaly towards negative x -axis,

$$\theta = -\theta_N \quad \text{or} \quad -(\theta_N + 360^\circ);$$

Major negative anomaly towards positive x -axis,

$$\theta = \theta_N - 180^\circ;$$

Major negative anomaly towards negative x -axis,

$$\theta = -(\theta_N + 180^\circ);$$

where θ_N is the θ value obtained from the nomogram (Fig. 2 or 3).

(ii) *Vertical fault model*: The depth (h) to the top edge of the fault may be evaluated using either of the following two relations

$$h = \sqrt{|x_M \cdot x_m| / (R + 1)} \quad (27)$$

or

$$h = \left| \frac{(x_M + x_m) \cdot \tan \theta}{R + 2} \right| \quad (28)$$

and the depth H to the bottom edge is obtained from the relation

$$H = (R + 1) \cdot h \quad (29)$$

Similar to the dike case, here also, one obtains, using Fig. 3 the θ value in the range 0° to 90° only. The actual θ value of the fault may be found using the same criteria given for the dike model.

In the case of induced magnetization, the dip (δ) of the dike/vertical fault may be found from the value of θ using its appropriate equivalent given in Table 1. If remanence is present, the dip of the body may be evaluated only when the direction of the remanent component is known.

4. Field examples

To test the applicability of this method the following two field examples are analysed.

Example 1: The first curve used for the analysis is a vertical field magnetic anomaly (Fig. 5) in Marcona district, Peru [Fig. 11 of GAY's (1963) paper]. The characteristic points are measured and the ratios D and A are found. In this case, $A > D$ and hence the curve belongs to a thick dike family. The ratios A and D are entered into the nomograms presented in Fig. 2 and the corresponding values of R and θ are noted. For this curve, the positive peak is dominant and is on the side of the negative x -axis. Hence $\theta = -49.5^\circ$. The parameters of the dike are evaluated using the analytical relations presented in the previous section. The results thus obtained are presented in Table 2 together with those obtained by GAY (1963) and KOULOMZINE *et al.* (1970) for direct comparison.

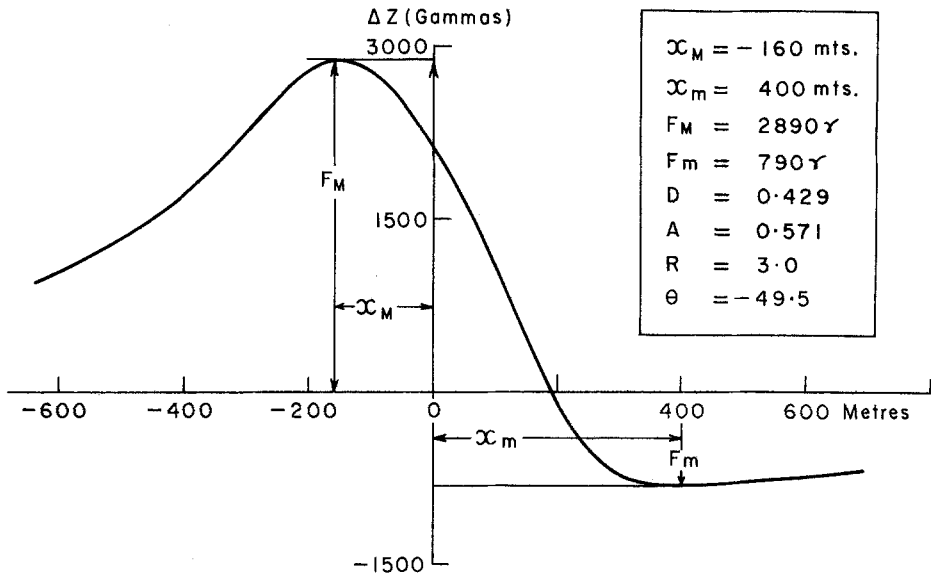


Figure 5

Analysis of the vertical field magnetic anomaly over Marcona district, Peru. The characteristic amplitudes, distances and the ratios are shown in the inset.

Table 2

Results of analysis of the vertical magnetic anomaly shown in Fig. 5

Parameter	Results obtained by		
	GAY (1963)	KOULOMZINE <i>et al.</i> (1970)	Present method
Depth (<i>h</i>) to top in metres	124.0	126.7	140.5
		135.5	140.3
Width (<i>2b</i>) in metres	372.0	411.9	421.5
		405.5	420.9
θ in degrees	-50	-50.13 -50.53	-49.5

Example 2: The second curve used for the analysis is a total field magnetic anomaly (Fig. 6) on the western margin of the Perth basin [Fig. 5 of QURESHI and NALAYE's (1978) paper]. Since the minimum appears to be disturbed, the curve has been extrapolated (dashed curve) towards the minimum using POWELL's (1967) technique. For this curve, $A < D$ which indicates that the anomaly curve belongs to a fault family. The ratios A and D are entered into the nomograms for the fault model (Fig. 3) and the corresponding values of R and θ are noted. For this curve, dominant positive is towards the positive x -axis. Hence $\theta = 45^\circ$ or -315° . The results (Table 3) of our interpretation are in close agreement with those obtained by QURESHI and NALAYE (1978).

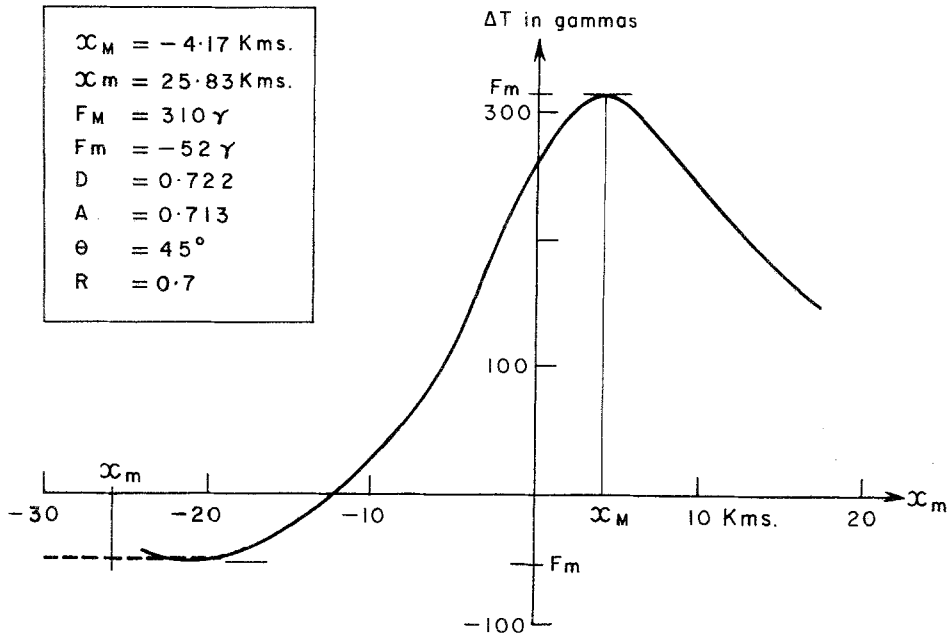


Figure 6

Analysis of the total field magnetic anomaly over the western margin of Perth Basin. The dashed curve is the extrapolated curve towards the minimum using POWELL's (1967) technique. The characteristic amplitudes, distances and the ratios are shown in the inset.

Table 3

Results of analysis of the total field magnetic anomaly shown in Fig. 6

Parameter	Results obtained by	
	QURESHI and NALAYE (1978)	Present method
Depth (<i>h</i>) to top in km	6.85	7.2
	6.30	7.9
Depth (<i>H</i>) to bottom in km	15.55	14.4
	16.50	15.7
<i>θ</i> in degrees	-330	-315

5. Limitations of the method

It is well known that the methods of interpretation based on a few characteristic points on the anomaly curve give poor results if the characteristic points are wrongly recognized or superposed by noise due to surrounding features. However, these methods are faster in application than the classical curve-matching techniques and give surprisingly good results in a large number of cases (AM, 1972).

The method presented in this paper, entirely depends on the positions of the origin, zero line, maximum and minimum points on the anomaly curve. If any error is associated in locating them, the same will be reflected in the results. However, this method is not applicable when the anomaly curve is either symmetric or antisymmetric due to the following reasons: When the anomaly curve is (a) symmetric (i.e., when $\theta = 0^\circ$), both the ratios D and A tend to unity and (b) antisymmetric (i.e., when $\theta = 90^\circ$), both D and A tend to zero. In these two cases, it may be seen from Figs. 2 and 3 that the nomograms for different values of R converge and hence a unique solution for R is not possible using these nomograms.

Using this method, the procedure for determining the depth and width (for dike)/bottom depth (for vertical fault) of the body is identical for both the cases of induced and remanent magnetization (if the remanent field remains constant in direction and magnitude throughout the body). However, the dip and thickness of the body may be determined only when the amplitude and direction of the remanent component are known.

Acknowledgments

We thank Dr P. V. Sanker Narayan, Assistant Director, NGRI, for his constant encouragement throughout this work. We thank the Director, NGRI, for his kind permission to publish this work. The draughting work of Mr G. Giridharan is deeply appreciated.

REFERENCES

- AM, K. (1972), *The Arbitrarily Magnetized Dike: Interpretation by Characteristics*, *Geoexploration* 10, 63–90.
- BEAN, R. J. (1966), *A Rapid Graphical Solution for the Aeromagnetic Anomaly of the Two-Dimensional Tabular Body*, *Geophysics* 31, 963–970.
- BRUCKSHAW, J. M., and KUNARATNAM, K. (1963), *The Interpretation of Magnetic Anomalies Due to Dykes*, *Geophys. Prospect.* 11, 509–522.
- GAY, S. P. (1963), *Standard Curves for Interpretation of Magnetic Anomalies Over Long Tabular Bodies*, *Geophysics* 28, 161–200.
- GRANT, F. S., and MARTIN, L. (1966), *Interpretation of Aeromagnetic Anomalies by the Use of Characteristic Curves*, *Geophysics* 31, 135–148.
- HOOD, P. (1964), *The Königsberger Ratio and the Dipping-Dike Equation*, *Geophys. Prospect.* 12, 440–456.
- KOULOMZINE, TH., LAMONTAGNE, Y., and NADEAU, A. (1970), *New Methods for the Direct Interpretation of Magnetic Anomalies Caused by Inclined Dikes of Infinite Length*, *Geophysics* 35, 812–830.
- MOO, J. K. C. (1965), *Analytical Aeromagnetic Interpretation: The Inclined Prism*, *Geophys. Prospect.* 13, 203–224.
- POWELL, D. W. (1967), *Fitting Observed Profiles to a Magnetized Dike or Fault-Step Model*, *Geophys. Prospect.* 15, 208–220.
- QURESHI, I. R., and NALAYE, A. M. (1978), *A Method for the Direct Interpretation of Magnetic Anomalies Caused by Two-Dimensional Vertical Faults*, *Geophysics* 43, 179–188.

(Received 19th January 1981, revised 10th July 1981)